Decays $\omega(782)$, $\phi(1020)\to 5\pi$ in the hidden local symmetry approach

N. N. Achasov* and A. A. Kozhevnikov†
Laboratory of Theoretical Physics, S. L. Sobolev Institute for Mathematics, 630090, Novosibirsk, Russian Federation
(Received 20 June 2003; published 28 October 2003)

The decays $\omega\to 2\pi^+2\pi^-\pi^0$ and $\omega\to\pi^+\pi^-3\pi^0$ are reconsidered in the hidden local symmetry approach (HLS) with added anomalous terms. The decay amplitudes are analyzed in detail, paying special attention to the Adler condition of the vanishing of the whole amplitude at a vanishing of momentum of any final pion. Combining the Okubo-Zweig-Iizuka rule applied to the five-pion final state with the Adler condition, we also calculate the $\phi\to 2\pi^+2\pi^-\pi^0$ and $\phi\to\pi^+\pi^-3\pi^0$ decay amplitudes. The partial widths of the above decays are evaluated, and the excitation curves in e^+e^- annihilation are obtained, assuming specific reasonable relations among the parameters characterizing the anomalous terms of the HLS Lagrangian. The evaluated branching ratios $B_{\phi\to\pi^+\pi^-3\pi^0}\approx 2\times 10^{-7}$ and $B_{\phi\to 2\pi^+2\pi^-\pi^0}\approx 7\times 10^{-7}$ are such that, with the luminosity $L=500$ pb^{-1} attained at the DAΦNE ϕ factory, one may already possess about 1685 events of the $\phi\to 5\pi$ decays.

DOI: 10.1103/PhysRevD.68.074009 PACS number(s): 13.30.Eg, 11.30.Rd, 12.39.Fe

I. INTRODUCTION

The purpose of the present paper is to calculate the branching ratios of the decays

$$\omega\to\pi^+\pi^-3\pi^0, \tag{1.1}$$

$$\omega\to 2\pi^+2\pi^-\pi^0, \tag{1.2}$$

$$\phi\to\pi^+\pi^-3\pi^0, \tag{1.3}$$

and

$$\phi\to 2\pi^+2\pi^-\pi^0, \tag{1.4}$$

in the framework of a chiral model for pseudoscalar and low lying vector mesons based on hidden local symmetry (HLS) [1,2]. This model incorporates vector mesons into chiral theory in a most elegant way. The fact is that the low energy theorems for anomalous processes such as, say, the decay $\pi^0\to\gamma\gamma$, are satisfied automatically in HLS. Since the general form of both the nonanomalous and anomalous parts of the Lagrangian is given in Refs. [1,2], we write down here the weak field limit of the above Lagrangian restricted to the subgroup $SU(2)\times U(1)$ with only the isovector $\boldsymbol{\pi}$, $\boldsymbol{\rho}$ and isoscalar ω mesons taken into account. Including the coupling of the $\phi(1020)$ meson with mesons composed of nonstrange quarks demands additional assumptions to be discussed below.

The nonanomalous part of the HLS Lagrangian (denoted as "nan") is obtained from the general expression of Refs. [1–3] and looks like

$$\begin{aligned}\mathcal{L}^{\rm nan}=&-\frac{1}{4}\boldsymbol{\rho}_{\mu\nu}^2-\frac{1}{4}\omega_{\mu\nu}^2+\frac{1}{2}ag^2f_\pi^2(\boldsymbol{\rho}_\mu^2+\omega_\mu^2)+\frac{1}{2}(\partial_\mu\boldsymbol{\pi})^2\\&-\frac{1}{2}m_\pi^2\boldsymbol{\pi}^2+\frac{m_\pi^2}{24f_\pi^2}\boldsymbol{\pi}^4+\frac{1}{2f_\pi^2}\left(\frac{a}{4}-\frac{1}{3}\right)[\boldsymbol{\pi}\times\partial_\mu\boldsymbol{\pi}]^2\\&+\frac{1}{2}ag\left(1-\frac{\boldsymbol{\pi}^2}{12f_\pi^2}\right)(\boldsymbol{\rho}_\mu\cdot[\boldsymbol{\pi}\times\partial_\mu\boldsymbol{\pi}]),\end{aligned} \tag{1.5}$$

where the dot $(\cdot)$ and cross $(\times)$ stand, respectively, for the scalar and vector products in the isotopic space,

$$\begin{aligned}\boldsymbol{\rho}_{\mu\nu}&=\partial_\mu\boldsymbol{\rho}_\nu-\partial_\nu\boldsymbol{\rho}_\mu+g[\boldsymbol{\rho}_\mu\times\boldsymbol{\rho}_\nu],\\ \omega_{\mu\nu}&=\partial_\mu\omega_\nu-\partial_\nu\omega_\mu\end{aligned} \tag{1.6}$$

are, respectively, the field strengths of the isovector field $\boldsymbol{\rho}_\mu$ and the isoscalar field ω_μ, g is the gauge coupling constant, $f_\pi=92.4$ MeV is the pion decay constant, and a is the HLS parameter. The boldface characters refer hereafter to vectors in isotopic space. As is clear from Eq. (1.5),

$$\begin{aligned}g_{\rho\pi\pi}&=\frac{1}{2}ag,\\ m_\rho^2&=ag^2f_\pi^2\end{aligned} \tag{1.7}$$

are the $\rho\pi\pi$ coupling constant and the ρ mass squared, respectively. The $\omega(782)$ is degenerate with ρ in the present model. Note that $a=2$, if one requires the universality condition $g=g_{\rho\pi\pi}$. Then the Kawarabayashi-Suzuki-Riazzuddin-Fayyazuddin relation [4] arises:

$$\frac{2g_{\rho\pi\pi}^2f_\pi^2}{m_\rho^2}=1, \tag{1.8}$$

which beautifully agrees with experiment. The $\rho\pi\pi$ cou-

*Electronic address: achasov@math.nsc.ru
†Electronic address: kozhev@math.nsc.ru

pling constant resulting from this relation is $g_{\rho\pi\pi}=5.9$.

To include the decays of the ω meson to the many pion states one should add the anomalous terms (denoted below as "an"). They are given in Refs. [1,2]. Since only strong decays will be of concern here, we omit the terms containing the electromagnetic field. Again, restricting ourselves to the weak field limit and to the ρ, ω, and π fields, we arrive at the expression

$$\mathcal{L}^{\rm an}=\frac{n_c g}{32\pi^2 f_\pi^3}(c_1-c_2-c_3)\varepsilon_{\mu\nu\lambda\sigma}\omega_\mu(\partial_\nu\boldsymbol{\pi}\cdot[\partial_\lambda\boldsymbol{\pi}\times\partial_\sigma\boldsymbol{\pi}])+\frac{n_c g}{128\pi^2 f_\pi^5}\left[-c_1+\frac{5}{3}(c_2+c_3)\right]\varepsilon_{\mu\nu\lambda\sigma}\omega_\mu(\partial_\nu\boldsymbol{\pi}\cdot[\partial_\lambda\boldsymbol{\pi}\times\partial_\sigma\boldsymbol{\pi}])\boldsymbol{\pi}^2$$
$$-\frac{n_c g^2 c_3}{8\pi^2 f_\pi}\varepsilon_{\mu\nu\lambda\sigma}\partial_\mu\omega_\nu\left\{(\boldsymbol{\rho}_\lambda\cdot\partial_\sigma\boldsymbol{\pi})+\frac{1}{6f_\pi^2}[(\boldsymbol{\rho}_\lambda\cdot\boldsymbol{\pi})(\boldsymbol{\pi}\cdot\partial_\sigma\boldsymbol{\pi})-\boldsymbol{\pi}^2(\boldsymbol{\rho}_\lambda\cdot\partial_\sigma\boldsymbol{\pi})]\right\}$$
$$-\frac{n_c g^2}{8\pi^2 f_\pi}(c_1+c_2-c_3)\varepsilon_{\mu\nu\lambda\sigma}\omega_\mu\left\{\frac{1}{4f_\pi^2}(\partial_\nu\boldsymbol{\pi}\cdot\boldsymbol{\rho}_\lambda)(\boldsymbol{\pi}\cdot\partial_\sigma\boldsymbol{\pi})-\frac{g}{4}([\boldsymbol{\rho}_\nu\times\boldsymbol{\rho}_\lambda]\cdot\partial_\sigma\boldsymbol{\pi})\right\}, \tag{1.9}$$

where $n_c=3$ is the number of colors, and $c_{1,2,3}$ are arbitrary constants multiplying three independent structures in the solution [1,2] of the Wess-Zumino anomaly equation [5]; the fourth constant c_4 multiplying the structure that includes the electromagnetic field, as explained above, is dropped. Our normalization of $c_{1,2,3}$ is in accord with Ref. [2]. As is evident from the second line of Eq. (1.9), the $\omega\rho\pi$ coupling constant is

$$g_{\omega\rho\pi}=-\frac{n_c g^2 c_3}{8\pi^2 f_\pi}. \tag{1.10}$$

Assuming

$$c_1-c_2-c_3=0, \tag{1.11}$$

i.e., the absence of the pointlike $\omega\to\pi^+\pi^-\pi^0$ amplitude, and using the $\omega\to\pi^+\pi^-\pi^0$ partial width to extract $g_{\omega\rho\pi}$ and the $\rho\to\pi^+\pi^-$ partial width and Eq. (1.7) to extract $g=g_{\rho\pi\pi}=6.00\pm0.01$ (assuming $a=2$), one finds

$$c_3=0.99\pm0.01, \tag{1.12}$$

where the errors come from the errors of the ω and ρ widths. Hereafter we use the particle parameters (masses, full and partial widths, etc.) taken from Ref. [6].

The remaining material of the paper is organized as follows. Section II is devoted to obtaining the $\omega\to\pi^+\pi^-3\pi^0$ and $\omega\to2\pi^+2\pi^-\pi^0$ decay amplitudes from the Lagrangians given by Eqs. (1.5) and (1.9) and verifying the Adler condition for their expressions. The results of the evaluation of the branching ratios at the ω pole position and the calculation of the excitation curves of the above decays in e^+e^- annihilation are given in Sec. III, imposing the natural constraints on the parameters $c_{1,2,3}$ characterizing the anomalous terms of the HLS Lagrangian. As is shown there, the branching ratios evaluated depend insignificantly on the exact form of the constraints. The reason for disagreement with our previous evaluations [7] of the branching ratios for the decays (1.1) and (1.2) is explained. In Sec. IV, guided by specific assumptions about how the Okubo-Zweig-Iizuka (OZI) rule is violated in the decays of ϕ mesons into states containing no particles with strangeness, the effective Lagrangian for the $\phi\to\pi^+\pi^-3\pi^0$ and $\phi\to2\pi^+2\pi^-\pi^0$ decay amplitudes is written. Under assumptions about the free parameters of this Lagrangian similar to those for $c_{1,2,3}$, the branching ratios and the e^+e^- annihilation excitation curves for the five-pion decays of the ϕ are given in the same section. Estimates of the number of events of the decays $\omega,\phi\to\pi^+\pi^-3\pi^0$ and $\omega,\phi\to2\pi^+2\pi^-\pi^0$ at the respective ω and ϕ peak positions and general conclusions about the possibilities of detecting the decays under consideration in e^+e^- annihilation are given in Sec. V. Kinematical relations ex-

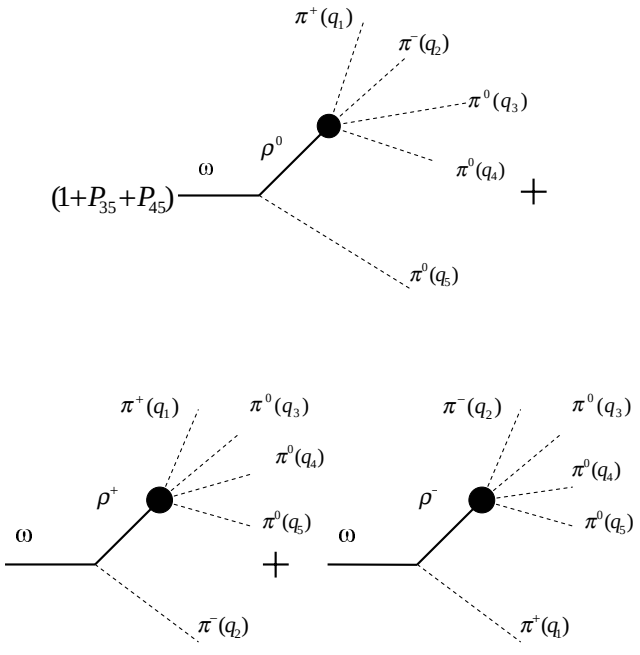

FIG. 1. The diagrams describing the amplitudes of the decay $\omega\to\pi^+\pi^-3\pi^0$ through the ρ intermediate state followed by the decay $\rho\to4\pi$. The shaded circles refer to the whole $\rho\to4\pi$ amplitudes.

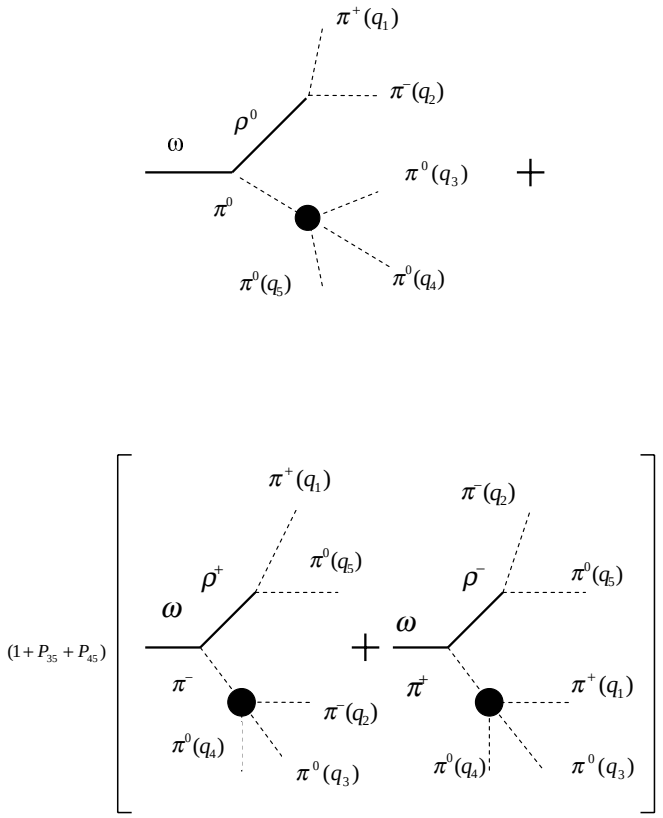

FIG. 2. The diagrams describing the amplitudes of the decay $\omega\to\pi^+\pi^-3\pi^0$ through the $\rho\pi$ intermediate state followed by the transitions $\rho\to 2\pi$ and $\pi\to 3\pi$. The shaded circles refer to the effective $\pi\to 3\pi$ vertices given by Eq. (2.2). Note that the non-π-pole term is included in the diagrams in Fig. 4 below.

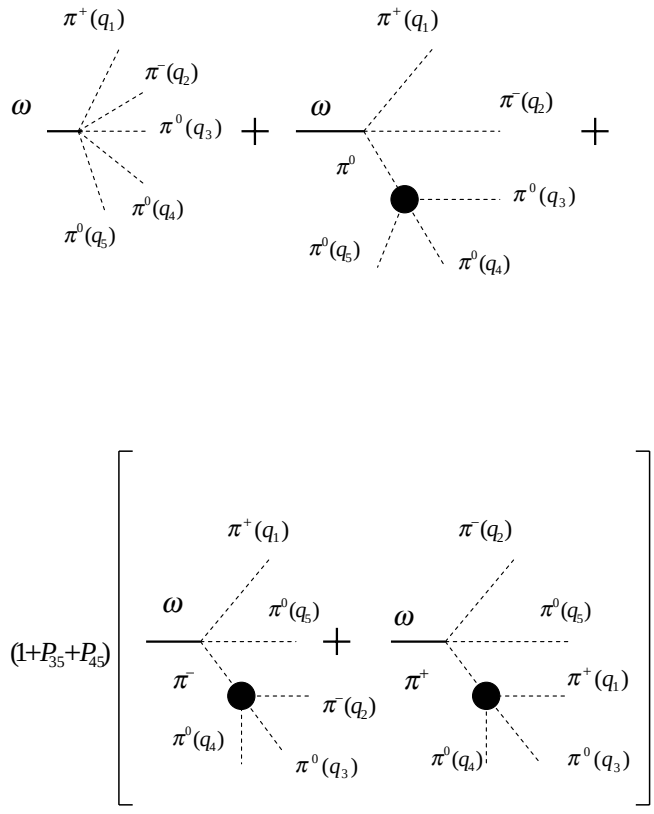

FIG. 3. The diagrams describing the contributions to the $\omega\to\pi^+\pi^-3\pi^0$ decay amplitude via pointlike vertices. The shaded circles refer to the effective $\pi\to 3\pi$ vertices given by Eq. (2.2).

pressing the Lorentz scalar products of the pion momenta through invariant Mandelstam-like variables, which are necessary for the phase space integration, are given in the Appendix.

II. THE $\omega\to\pi^+\pi^-3\pi^0$ AND $\omega\to 2\pi^+2\pi^-\pi^0$ DECAY AMPLITUDES

In this section, we obtain the $\omega\to\pi^+\pi^-3\pi^0$ and $\omega\to 2\pi^+2\pi^-\pi^0$ decay amplitudes and study their Adler limit, i.e., the limit at vanishing four-momentum of any final pion. Our notation for the Lorentz scalar product of two different four-vectors a and b is $(a,b)=a_0b_0-(\mathbf{a}\cdot\mathbf{b})$, while the Lorentz square is denoted as usual as a^2. We divide the presentation into two subsections for each above mentioned isotopic configuration of the final state pions.

A. The $\omega\to\pi^+\pi^-3\pi^0$ final state

The diagrams for the amplitude of the decay

$$\omega_q\to\pi^+_{q_1}\pi^-_{q_2}\pi^0_{q_3}\pi^0_{q_4}\pi^0_{q_5}, \tag{2.1}$$

where we explicitly label each particle in the reaction by its four-momentum, are shown in Figs. 1–4. Let us give the expressions corresponding to them. The upper index (n) (indicating *neutral*, because three neutral pions are in the final state) will designate this particular isotopic state. The amplitude corresponding to Fig. 1 includes the four-pion decay of the intermediate ρ meson which was extensively discussed in, e.g., [7]. The Lagrangian due to Weinberg [8] was used in Ref. [7] to find the expressions for the $\rho\to 4\pi$ decay amplitudes. This Lagrangian is different in coefficients as compared to Eq. (1.5) above. However, one can show by direct computation that due to the well known parameter independence the $\rho\to 4\pi$ decay amplitudes resulting from the above Lagrangians coincide. The reason is that the terms proportional to $D_\pi(k)$ in the $\pi\to 3\pi$ amplitudes,

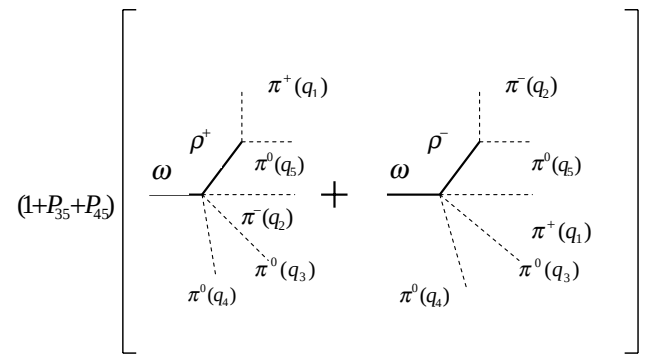

FIG. 4. The contributions to the $\omega\to\pi^+\pi^-3\pi^0$ decay amplitude arising due to the chiral vertex $\omega\to\rho 3\pi$.

$$M(\pi_k^+ \to \pi_{q_1}^+ \pi_{q_2}^+ \pi_{q_3}^-)$$
$$= \frac{1}{2f_\pi^2}(1+\hat{P}_{12})\Big[-a(q_1,q_3)+(a-2)(q_1,q_2)$$
$$+ am_\rho^2 \frac{(q_2,q_3-q_1)}{D_\rho(q_1+q_3)} - \frac{1}{3}D_{\pi^+}(k)\Big],$$

$$M(\pi_k^+ \to \pi_{q_1}^+ \pi_{q_3}^0 \pi_{q_4}^0)$$
$$= \frac{1}{2f_\pi^2}(1+\hat{P}_{34})\Big[-(a-1)(q_3,q_4)+(a-2)(q_1,q_3)$$
$$+ am_\rho^2 \frac{(q_4,q_3-q_1)}{D_\rho(q_1+q_3)} - \frac{1}{6}D_{\pi^+}(k)\Big],$$

$$M(\pi_k^0 \to \pi_{q_1}^+ \pi_{q_2}^- \pi_{q_5}^0)$$
$$= \frac{1}{2f_\pi^2}(1+\hat{P}_{12})\Big[-(a-1)(q_1,q_2)+(a-2)(q_1,q_5)$$
$$+ am_\rho^2 \frac{(q_2,q_1-q_5)}{D_\rho(q_1+q_5)} - \frac{1}{6}D_{\pi^0}(k)\Big],$$

$$M(\pi^0 \to \pi_{q_3}^0 \pi_{q_4}^0 \pi_{q_5}^0) = \frac{m_{\pi^0}^2}{f_\pi^2}, \qquad (2.2)$$

which vanish on the pion mass shell, give the non-π-pole terms in the $\rho \to 2\pi \to 4\pi$ amplitude. When added to the pointlike $\rho \to 4\pi$ amplitude, they make their sum parameter independent. The same occurs with such terms in the expression derived from Fig. 2 below, which should be added to the expression derived from Fig. 4. The final expressions for the full $\omega \to \pi^+\pi^- 3\pi^0$ decay amplitude will be given below. Hereafter $\hat{P}_{ij}$ is the operator of permutation of the pion momenta q_i and q_j,

$$D_\rho(k) = m_\rho^2 - k^2 - i\sqrt{k^2}\Gamma_{\rho\to\pi^+\pi^-}(k^2),$$

$$\Gamma_{\rho\to\pi^+\pi^-}(k^2) = \frac{g_{\rho\pi\pi}^2}{48\pi k^2}(k^2-4m_{\pi^+}^2)^{3/2} \qquad (2.3)$$

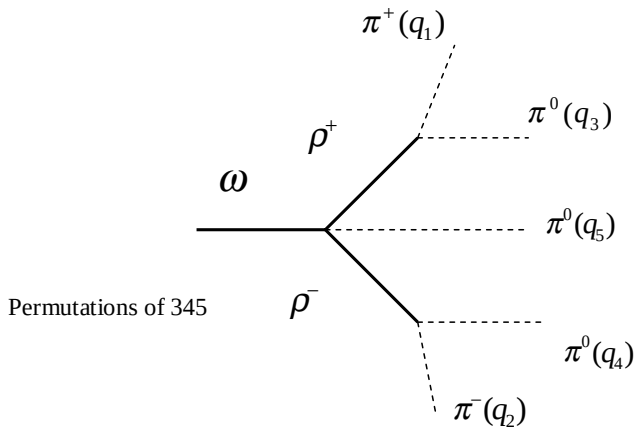

FIG. 5. The contributions to the $\omega \to \pi^+\pi^- 3\pi^0$ decay amplitude via the intermediate state with two ρ mesons. Total number of diagrams of this kind is $3! = 6$.

are the inverse propagator of the ρ meson and its two-pion decay width, respectively, and

$$D_{\pi^{+,0}}(k) = m_{\pi^{+,0}}^2 - k^2 \qquad (2.4)$$

is the inverse propagator of the $\pi^{\pm,0}$ meson. The following shorthand notation for inverse propagators of the particle A will be used:

$$D_{Aab} \equiv D_A(q_a+q_b), \quad D_{Aabc} \equiv D_A(q_a+q_b+q_c). \quad (2.5)$$

Let us give the expression for each diagram in Figs. 1–5. Choosing q_μ, ϵ_μ for the four-momentum and four-vector of polarization of the ω, one obtains

$$M_1^{(n)} = \frac{g_{\omega\rho\pi}g_{\rho\pi\pi}}{f_\pi^2}\varepsilon_{\mu\nu\lambda\sigma}q_\mu\epsilon_\nu\Big[(1+\hat{P}_{35}+\hat{P}_{45})\frac{q_{5\lambda}}{D_\rho(q-q_5)}$$
$$\times J_\sigma(\rho^0 \to \pi_{q_1}^+\pi_{q_2}^-\pi_{q_3}^0\pi_{q_4}^0) + (1-\hat{P}_{12})\frac{q_{2\lambda}}{D_\rho(q-q_2)}$$
$$\times J_\sigma(\rho^+ \to \pi_{q_1}^+\pi_{q_3}^0\pi_{q_4}^0\pi_{q_5}^0)\Big] \qquad (2.6)$$

for the diagrams of Fig. 1. The $\rho \to 4\pi$ decay currents in Eq. (2.6) are [7]

$$J_\sigma(\rho^0 \to \pi_{q_1}^+\pi_{q_2}^-\pi_{q_3}^0\pi_{q_4}^0) = (1-\hat{P}_{12})(1+\hat{P}_{34})\Bigg(q_{1\sigma}\Bigg\{-\frac{1}{4}+\frac{1}{D_{\pi^+234}}\Bigg[(q_3,q_4-2q_2)+a(q_3,q_2-q_4)\Bigg(\frac{m_\rho^2}{D_{\rho24}}-1\Bigg)\Bigg]\Bigg\}$$
$$+\frac{m_\rho^2}{2D_{\rho13}D_{\rho24}}[(q_3+q_1)_\sigma(q_1-q_3,q_2-q_4)+2(q_3-q_1)_\sigma(q_1+q_3,q_2-q_4)]$$
$$+2\Bigg(\frac{n_c g^2 c_3}{8\pi^2}\Bigg)^2\frac{1}{D_{\omega123}}\Bigg(\frac{1}{D_{\rho12}}+\frac{1}{D_{\rho13}}+\frac{1}{D_{\rho23}}+3\frac{c_1-c_2-c_3}{2c_3m_\rho^2}\Bigg)\{q_{1\sigma}[(k,q_2)(q_3,q_4)$$
$$-(k,q_3)(q_2,q_4)]+q_{3\sigma}(k,q_1)(q_2,q_4)\}\Bigg) \qquad (2.7)$$

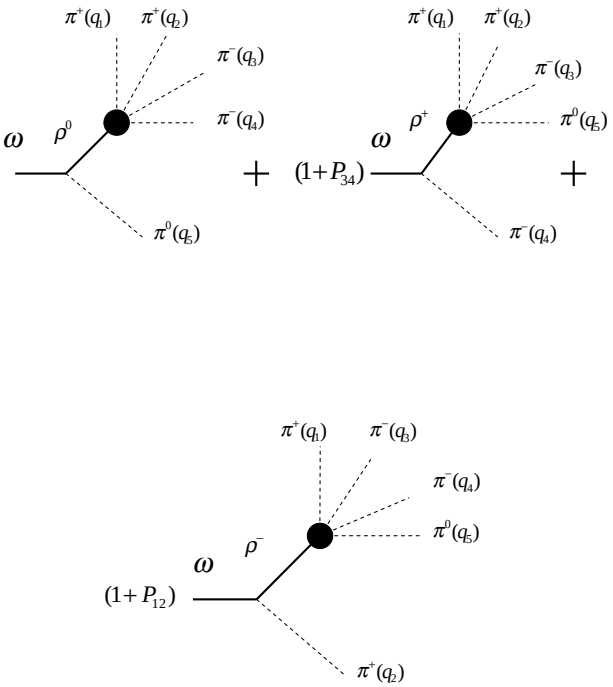

FIG. 6. The diagrams describing the amplitudes of the decay $\omega\to 2\pi^+ 2\pi^- \pi^0$ through the ρ intermediate state followed by the decay $\rho\to 4\pi$. The shaded circles refer to the whole $\rho\to 4\pi$ amplitudes.

(with $k=q_1+q_2+q_3+q_4$), where

$$D_{\omega abc}\equiv D_\omega(q_a+q_b+q_c)=m_\omega^2-(q_a+q_b+q_c)^2-im_\omega\Gamma_\omega \tag{2.8}$$

is the inverse propagator of the ω (we take the fixed width approximation for the ω meson because the ω resonance is narrow), and

$$\begin{aligned}J_\sigma(\rho^+\to\pi^+_{q_1}\pi^0_{q_3}\pi^0_{q_4}\pi^0_{q_5})&=(1+\hat P_{34}+\hat P_{35})\left\{\frac{1}{3}q_{1\sigma}\left(1-\frac{2m_{\pi^0}^2}{D_{\pi^0 345}}\right)\right.\\&+\frac{q_{3\sigma}}{D_{\pi^+145}}(1+\hat P_{45})\left[(q_4,q_5-2q_1)\right.\\&\left.\left.+a(q_4,q_5-q_1)\left(\frac{m_\rho^2}{D_{\rho 15}}-1\right)\right]\right\}.\end{aligned} \tag{2.9}$$

The expression for the diagrams in Fig. 2 is

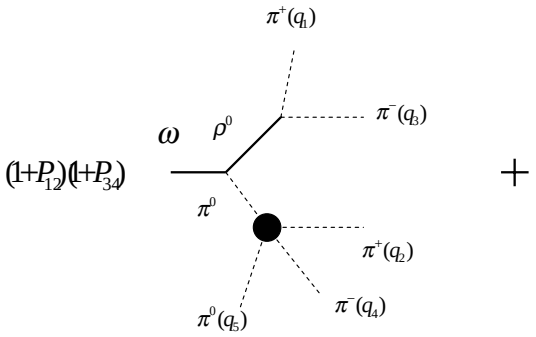

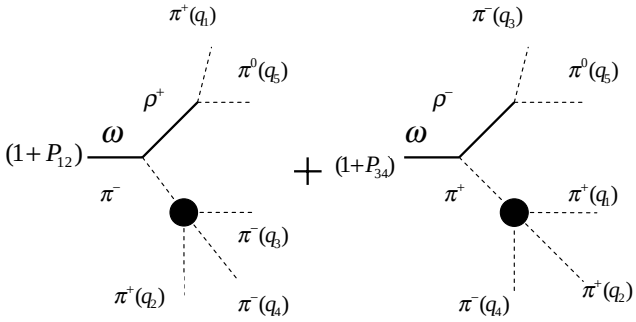

FIG. 7. The diagrams describing the amplitudes of the decay $\omega\to 2\pi^+ 2\pi^- \pi^0$ through the $\rho\pi$ intermediate state followed by the transitions $\rho\to 2\pi$ and $\pi\to 3\pi$. The shaded circles refer to the effective $\pi\to 3\pi$ vertices given by Eq. (2.2). Note that the non-π-pole term is included in the first pair of diagrams in Fig. 9 below.

$$\begin{aligned}M_2^{(n)}=&-\frac{g_{\omega\rho\pi}g_{\rho\pi\pi}}{f_\pi^2}(1-\hat P_{12})(1+\hat P_{35}+\hat P_{45})(1+\hat P_{34})\\&\times\varepsilon_{\mu\nu\lambda\sigma}q_\mu\epsilon_\nu\left\{\frac{q_{1\lambda}q_{5\sigma}}{D_{\rho 15}D_{\pi^+234}}\left[(q_3,q_4-2q_2)\right.\right.\\&\left.\left.+a(q_3,q_2-q_4)\left(\frac{m_\rho^2}{D_{\rho 24}}-1\right)\right]-\frac{q_{1\lambda}q_{2\sigma}m_{\pi^0}^2}{6D_{\rho 12}D_{\pi^0 345}}\right\}.\end{aligned} \tag{2.10}$$

The expression for the diagrams in Fig. 3 is

$$\begin{aligned}M_3^{(n)}=&\frac{n_c g}{32\pi^2 f_\pi^5}(1-\hat P_{12})(1+\hat P_{35}+\hat P_{45})\varepsilon_{\mu\nu\lambda\sigma}q_\mu\epsilon_\nu\\&\times\left(\frac{4c_1-5(c_2+c_3)}{3}q_{1\lambda}q_{2\sigma}+3(c_1-c_2-c_3)\right.\\&\times(1+\hat P_{34})\left\{\frac{q_{1\lambda}q_{5\sigma}}{D_{\pi^+234}}\left[(q_3,q_4-2q_2)+a(q_3,q_2-q_4)\right.\right.\\&\left.\left.\left.\times\left(\frac{m_\rho^2}{D_{\rho 24}}-1\right)\right]+\frac{q_{1\lambda}q_{2\sigma}}{3D_{\pi^0 345}}(q_3,q_4)\right\}\right).\end{aligned} \tag{2.11}$$

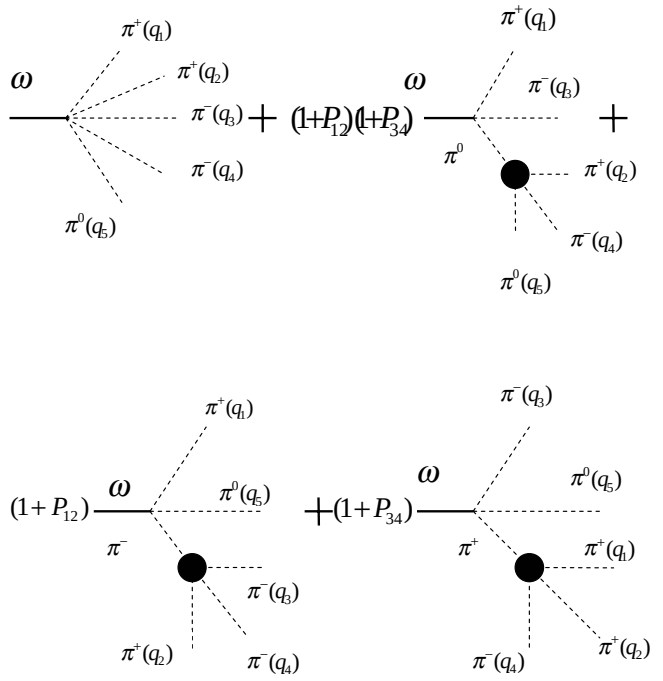

FIG. 8. The diagrams describing the contributions to the $\omega \to 2\pi^+ 2\pi^- \pi^0$ decay amplitude via pointlike vertices. The shaded circles refer to the effective $\pi \to 3\pi$ vertices given by Eq. (2.2).

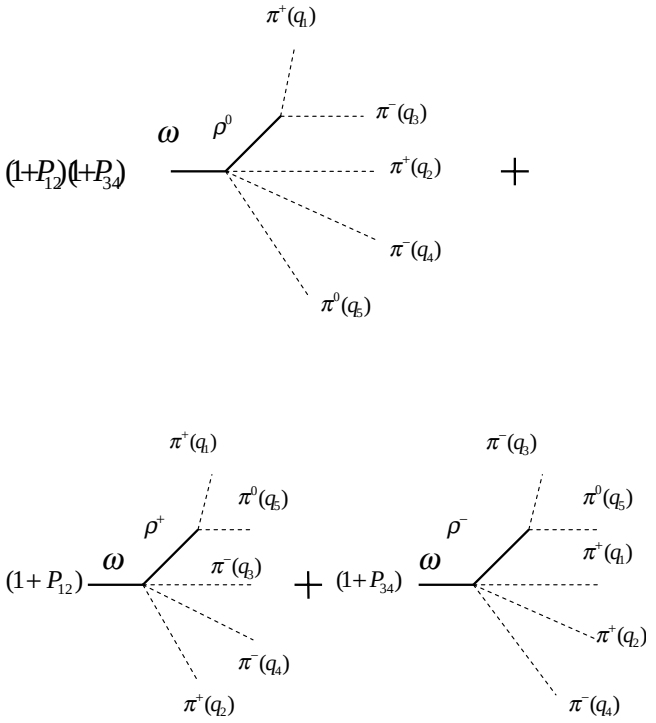

FIG. 9. The contributions to the $\omega \to 2\pi^+ 2\pi^- \pi^0$ decay amplitude arising due to the chiral $\omega \to \rho 3\pi$ vertex.

Notice the relation

$$\frac{n_c g}{32\pi^2 f_\pi^5} = -\frac{g_{\omega\rho\pi} g_{\rho\pi\pi}}{f_\pi^2} \cdot \frac{1}{2c_3 m_\rho^2}, \tag{2.12}$$

which is useful for easier comparison of the present contribution with others. The expression for the diagrams of Figs. 4 and 5 are, respectively,

$$M_4^{(n)} = -\frac{g_{\omega\rho\pi} g_{\rho\pi\pi}}{f_\pi^2}(1-\hat{P}_{12})(1+\hat{P}_{35}+\hat{P}_{45})\varepsilon_{\mu\nu\lambda\sigma} \times \frac{\epsilon_\nu (q_1-q_5)_\lambda}{2D_{\rho 15}}\left[q_\mu q_{2\sigma} - \frac{c_1+c_2-c_3}{2c_3} q_{2\mu}(q_3+q_4)_\sigma \right] \tag{2.13}$$

and

$$M_5^{(n)} = \frac{g_{\omega\rho\pi} g_{\rho\pi\pi} m_\rho^2}{f_\pi^2} \cdot \frac{c_1+c_2-c_3}{4c_3}(1-\hat{P}_{12})(1+\hat{P}_{35}+\hat{P}_{45}) \times \varepsilon_{\mu\nu\lambda\sigma} \frac{\epsilon_\nu (q_1-q_3)_\mu (q_2-q_4)_\lambda q_{5\sigma}}{D_{\rho 13} D_{\rho 24}}. \tag{2.14}$$

The full $\omega \to \pi^+\pi^- 3\pi^0$ decay amplitude is

$$M(\omega_q \to \pi^+_{q_1} \pi^-_{q_2} \pi^0_{q_3} \pi^0_{q_4} \pi^0_{q_5}) = M_1^{(n)} + M_2^{(n)} + M_3^{(n)} + M_4^{(n)} + M_5^{(n)}. \tag{2.15}$$

Since the expression for the amplitude is very cumbersome, one should invoke a method to control the calculations. We take the Adler condition as the method of this control.

1. Verifying the Adler condition for the $\omega \to \pi^+\pi^- 3\pi^0$ decay amplitude

The Adler condition is the condition of vanishing of the amplitude of the process with soft pions when the four-momentum of any pion is vanishing. Pions emitted in the decay $\omega \to 5\pi$ [7] are truly soft, because they possess the typical momentum $|\mathbf{q}_\pi| \simeq 0.5 m_\pi$. To verify the Adler condition, we set any particular pion momentum to zero. The correct expression for the amplitude should then vanish.

(i) $q_1 = 0$. The contributions of the diagrams Fig. 3, 4, and 5 vanish; the contributions of the diagrams Fig. 1 and 2 are equal in magnitude but opposite in sign, and hence they are canceled. The Adler condition is satisfied. The case $q_2 = 0$ is obtained from the case $q_1 = 0$ by the permutation property [see the operator $1 - \hat{P}_{12}$ in front of each expression in Eqs. (2.6), (2.7), (2.10), (2.11), (2.13), and (2.14)].

(ii) $q_3 = 0$. Here the situation is more subtle. Let us represent the amplitude at $q_3 = 0$ in the form

$$M^{(n)}(q_3 = 0) = -\frac{g_{\omega\rho\pi} g_{\rho\pi\pi}}{f_\pi^2}(1-\hat{P}_{12})(1+\hat{P}_{45}) \times \epsilon_{\mu\nu\lambda\sigma} \epsilon_\nu T_{\mu\lambda\sigma}.$$

Then one obtains the following contributions to the tensor $T_{\mu\lambda\sigma}$ from the diagrams of Fig. 1–5, respectively:

$$T^{(1)}_{\mu\lambda\sigma}=\frac{q_\mu(q_1-q_4)_\lambda q_{5\sigma}}{2D_{\rho 14}},$$

$$T^{(2)}_{\mu\lambda\sigma}=\frac{q_\mu q_{1\lambda} q_{4\sigma}}{D_{\rho 14}},$$

$$T^{(3)}_{\mu\lambda\sigma}=-\frac{1}{4m_\rho^2}\left(q_\mu q_{1\lambda} q_{2\sigma}+\frac{c_1+c_2-c_3}{c_3}\cdot q_{1\mu} q_{2\lambda} q_{4\sigma}\right),$$

$$T^{(4)}_{\mu\lambda\sigma}=\frac{1}{6}q_\mu\left[\frac{3q_{1\lambda}q_{2\sigma}}{2m_\rho^2}+\frac{(q_1-q_4)_\lambda(2q_2-q_5)_\sigma-2q_{1\lambda}q_{4\sigma}}{D_{\rho 14}}\right]$$
$$-\frac{c_1+c_2-c_3}{4c_3}\left[\frac{q_{2\mu}(q_1-q_4)_\lambda q_{5\sigma}}{D_{\rho 14}}-\frac{q_{1\mu}q_{2\lambda}q_{4\sigma}}{m_\rho^2}\right],$$

$$T^{(5)}_{\mu\lambda\sigma}=\frac{c_1+c_2-c_3}{4c_3}\cdot\frac{q_{2\mu}(q_1-q_4)_\lambda q_{5\sigma}}{D_{\rho 14}}. \tag{2.16}$$

In the above formulas, the superscript indicates the label of the corresponding figure. Note that when obtaining the contribution $T^{(3)}_{\mu\lambda\sigma}$ the relation Eq. (2.12) is essential. As is seen from Eq. (2.16), the terms with the factor $(c_1+c_2-c_3)$ and without such a factor are canceled separately in the sum. Let us check this for the terms proportional to $q_\mu/6D_{\rho 14}$. One has for the sum of these terms $2(q_1-q_4)_\lambda(q_2+q_5)_\sigma+4q_{1\lambda}q_{4\sigma}$. Using the four-momentum conservation and taking into account the tensor $\epsilon_{\mu\nu\lambda\sigma}$, one can see that the above momentum combination vanishes. Hence, the Adler condition is also satisfied in the case $q_3=0$. The cases $q_{4,5}=0$ are obtained from this case by Bose symmetry.

B. The $\omega\to 2\pi^+2\pi^-\pi^0$ final state

The diagrams for the amplitude of the decay

$$\omega_q\to\pi^+_{q_1}\pi^+_{q_2}\pi^-_{q_3}\pi^-_{q_4}\pi^0_{q_5}, \tag{2.17}$$

where the particles are labeled by their four-momenta, are shown in Figs. 6–10. Let us give the expressions corresponding to them. The superscript (c) (denoting *charged*, because most pions in the final state are charged) will designate this particular isotopic state. The expression for the diagrams of Fig. 6 looks like

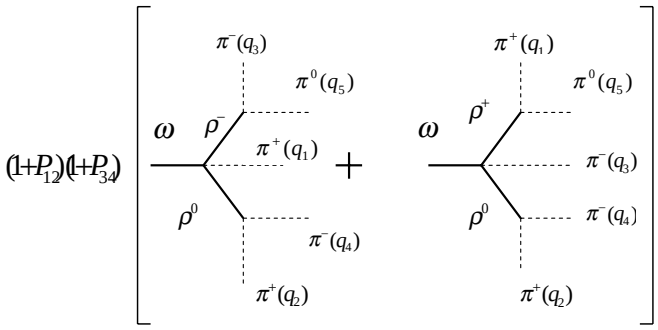

FIG. 10. The contributions to the $\omega\to 2\pi^+2\pi^-\pi^0$ decay amplitude via the intermediate state with two ρ mesons.

$$M^{(c)}_1=\frac{g_{\omega\rho\pi}g_{\rho\pi\pi}}{f_\pi^2}\varepsilon_{\mu\nu\lambda\sigma}q_\mu\epsilon_\nu\left[\frac{q_{5\lambda}}{D_\rho(q-q_5)}J_\sigma\right.$$
$$\times(\rho^0\to\pi^+_{q_1}\pi^+_{q_2}\pi^-_{q_3}\pi^-_{q_4})+(1+\hat P_{34})\frac{q_{4\lambda}}{D_\rho(q-q_4)}J_\sigma$$
$$\times(\rho^+\to\pi^+_{q_1}\pi^+_{q_2}\pi^-_{q_3}\pi^0_{q_5})+(1+\hat P_{12})\frac{q_{2\lambda}}{D_\rho(q-q_2)}J_\sigma$$
$$\left.\times(\rho^-\to\pi^+_{q_1}\pi^-_{q_3}\pi^-_{q_4}\pi^0_{q_5})\right]. \tag{2.18}$$

Here the currents responsible for the four-pion decay of the intermediate ρ meson are the following [7]:

$$J_\sigma(\rho^0\to\pi^+_{q_1}\pi^+_{q_2}\pi^-_{q_3}\pi^-_{q_4})$$
$$=(1+\hat P_{12})(1+\hat P_{34})(1-\hat P_{13}\hat P_{24})\left(q_{1\sigma}\left\{-\frac{1}{2}+\frac{1}{D_{\pi^+234}}\right.\right.$$
$$\left.\left.\times\left[a(q_3,q_2-q_4)\left(\frac{m_\rho^2}{D_{\rho 24}}-1\right)-2(q_3,q_4)\right]\right\}\right) \tag{2.19}$$

and

$$J_\sigma(\rho^+\to\pi^+_{q_1}\pi^+_{q_2}\pi^-_{q_3}\pi^0_{q_5})=(1+\hat P_{12})\left\{\frac{1}{2}(q_1-q_5)_\sigma-(1+\hat P_{23})\frac{q_{1\sigma}}{D_{\pi^0 135}}\left[(q_2,q_3-2q_5)+a(q_2,q_3-q_5)\left(\frac{m_\rho^2}{D_{\rho 35}}-1\right)\right]\right.$$
$$+\frac{q_{5\sigma}}{D_{\pi^+123}}\left[-2(q_1,q_2)+a(q_1,q_3-q_2)\left(\frac{m_\rho^2}{D_{\rho 23}}-1\right)\right]+(1-\hat P_{35})[2(q_1-q_5)_\sigma(q_1+q_5,q_2-q_3)$$
$$-(q_1+q_5)_\sigma(q_1-q_5,q_2-q_3)]\frac{m_\rho^2}{2D_{\rho 15}D_{\rho 23}}+\frac{2}{D_{\omega 135}}\left(\frac{n_c g^2 c_3}{8\pi^2}\right)^2[q_{1\sigma}(1-\hat P_{35})(k,q_3)(q_2,q_5)$$
$$+q_{3\sigma}(1-\hat P_{15})(k,q_5)(q_1,q_2)+q_{5\sigma}(1-\hat P_{13})(k,q_1)(q_2,q_3)]$$
$$\left.\times\left(\frac{1}{D_{\rho 13}}+\frac{1}{D_{\rho 15}}+\frac{1}{D_{\rho 33}}+\frac{c_1-c_2-c_3}{2c_3m_\rho^2}\right)\right\}, \tag{2.20}$$

where $k=q_1+q_2+q_3+q_5$. The expression for $J_\sigma(\rho^-\to\pi^+_{q_1}\pi^-_{q_3}\pi^-_{q_4}\pi^0_{q_5})$ is obtained from Eq. (2.20) by the replacements $q_1\leftrightarrow q_3$, $q_2\to q_4$, and by inverting an overall sign. The expression for the contribution of the diagrams of Fig. 7 is

$$M_2^{(c)}=\frac{g_{\omega\rho\pi}g_{\rho\pi\pi}}{f_\pi^2}(1+\hat P_{12})(1+\hat P_{34})\varepsilon_{\mu\nu\lambda\sigma}q_\mu\epsilon_\nu\Bigg\{(1+\hat P_{24})\frac{q_{1\lambda}q_{3\sigma}}{D_{\rho13}D_{\pi^0245}}\Bigg[(q_2,q_4-2q_5)+a(q_2,q_4-q_5)\left(\frac{m_\rho^2}{D_{\rho45}}-1\right)\Bigg]$$
$$-(1-\hat P_{13}\hat P_{24})\frac{q_{1\lambda}q_{5\sigma}}{D_{\rho15}D_{\pi^+234}}\Bigg[-2(q_3,q_4)+a(q_3,q_2-q_4)\left(\frac{m_\rho^2}{D_{\rho24}}-1\right)\Bigg]\Bigg\}. \tag{2.21}$$

The expression for the contribution of the diagrams of Fig. 8 looks like

$$M_3^{(c)}=\frac{n_c g}{32\pi^2 f_\pi^5}(1+\hat P_{12})(1+\hat P_{34})\varepsilon_{\mu\nu\lambda\sigma}q_\mu\epsilon_\nu\Bigg(\frac{4c_1-5(c_2+c_3)}{3}\cdot q_{1\lambda}q_{3\sigma}+3(c_1-c_2-c_3)\Bigg\{(1-\hat P_{14}\hat P_{23})\frac{q_{1\lambda}q_{5\sigma}}{D_{\pi^+234}}$$
$$\times\Bigg[-2(q_3,q_4)+a(q_3,q_2-q_4)\left(\frac{m_\rho^2}{D_{\rho24}}-1\right)\Bigg]-\frac{q_{1\lambda}q_{3\sigma}}{D_{\pi^0245}}(1+\hat P_{24})\Bigg[(q_2,q_4-2q_5)+a(q_2,q_4-q_5)\left(\frac{m_\rho^2}{D_{\rho45}}-1\right)\Bigg]\Bigg\}\Bigg). \tag{2.22}$$

Again, the relation Eq. (2.12) is necessary in verifying the Adler condition below. The expression for the contribution of the diagrams of Fig. 9 is

$$M_4^{(c)}=\frac{g_{\omega\rho\pi}g_{\rho\pi\pi}}{f_\pi^2}(1+\hat P_{12})(1+\hat P_{34})\varepsilon_{\mu\nu\lambda\sigma}\epsilon_\nu\Bigg\{\frac{1}{2}q_\mu\Bigg[\frac{(q_1-q_3)_\lambda q_{5\sigma}}{D_{\rho13}}+(1-\hat P_{13}\hat P_{24})\frac{q_{1\lambda}q_{5\sigma}+\frac{1}{2}(q_1-q_5)_\lambda q_{2\sigma}}{D_{\rho15}}\Bigg]$$
$$-\frac{c_1+c_2-c_3}{4c_3}\Bigg[\frac{q_{5\mu}(q_1-q_3)_\lambda(q_2+q_4)_\sigma}{D_{\rho13}}+(1-\hat P_{13}\hat P_{24})\frac{q_{1\mu}(q_3-q_5)_\lambda q_{4\sigma}}{D_{\rho35}}\Bigg]\Bigg\}. \tag{2.23}$$

Finally, the amplitude resulting from the diagrams of Fig. 10 is

$$M_5^{(c)}=-\frac{g_{\omega\rho\pi}g_{\rho\pi\pi}m_\rho^2}{f_\pi^2}\cdot\left(\frac{c_1+c_2-c_3}{4c_3}\right)(1+\hat P_{12})(1+\hat P_{34})$$
$$\times(1+\hat P_{24})\varepsilon_{\mu\nu\lambda\sigma}\epsilon_\nu\frac{(q_1-q_3)_\mu q_{4\lambda}(q_2-q_5)_\sigma}{D_{\rho13}D_{\rho25}}. \tag{2.24}$$

Notice that the product of the operators $(1+\hat P_{12})(1+\hat P_{34})$ makes evident the Bose symmetry of the full $\omega\to2\pi^+2\pi^-\pi^0$ decay amplitude,

$$M(\omega_q\to\pi^+_{q_1}\pi^+_{q_2}\pi^-_{q_3}\pi^-_{q_4}\pi^0_{q_5})$$
$$=M_1^{(c)}+M_2^{(c)}+M_3^{(c)}+M_4^{(c)}+M_5^{(c)}. \tag{2.25}$$

1. Verifying the Adler condition for the $\omega\to2\pi^+2\pi^-\pi^0$ decay amplitude

Let us write down the Adler limits of all the above contributions to the $\omega\to2\pi^+2\pi^-\pi^0$ decay amplitudes. As an example, the case $q_1=0$ is considered in detail. Representing the total amplitude Eq. (2.25) in this limit as

$$M^{(c)}(q_1=0)=\frac{g_{\omega\rho\pi}g_{\rho\pi\pi}}{f_\pi^2}(1+\hat P_{34})\varepsilon_{\mu\nu\lambda\sigma}\epsilon_\nu T_{\mu\lambda\sigma},$$

one has the following expressions for the diagrams of Figs. 6–10, respectively:

$$T^{(6)}_{\mu\lambda\sigma}(q_1=0)=\frac{1}{2}(1-\hat P_{35})q_\mu\Bigg[\frac{q_{4\lambda}(q_2-q_5)_\sigma}{D_{\rho25}}+\frac{q_{2\lambda}q_{3\sigma}}{D_{\rho35}}\Bigg],$$

$$T^{(7)}_{\mu\lambda\sigma}(q_1=0)=(1-\hat P_{35})\frac{q_\mu q_{2\lambda}q_{3\sigma}}{D_{\rho23}},$$

$$T^{(8)}_{\mu\lambda\sigma}(q_1=0)=-\left(2+\frac{c_1+c_2-c_3}{c_3}\right)\frac{q_\mu q_{2\lambda}q_{5\sigma}}{4m_\rho^2},$$

$$T^{(9)}_{\mu\lambda\sigma}(q_1=0)=\frac{1}{6}q_\mu\Bigg[\frac{-2q_{2\lambda}q_{3\sigma}+(q_2-q_3)_\lambda(2q_5-q_4)_\sigma}{D_{\rho35}}$$
$$-\frac{4q_{3\lambda}q_{5\sigma}+(q_3-q_5)_\lambda(2q_4-q_2)_\sigma}{D_{\rho23}}$$
$$+q_{2\lambda}q_{5\sigma}\left(\frac{3}{D_{\rho25}}+\frac{3}{m_\rho^2}\right)\Bigg]$$
$$+\frac{c_1+c_2-c_3}{4c_3}\Bigg[\frac{q_\mu q_{2\lambda}q_{5\sigma}}{m_\rho^2}$$
$$+(1-\hat P_{24}\hat P_{35})\frac{q_{3\mu}(q_4-q_5)_\lambda q_{2\sigma}}{D_{\rho45}}\Bigg],$$

$$T^{(10)}_{\mu\lambda\sigma}(q_1=0)=-\frac{c_1+c_2-c_3}{4c_3}(1-\hat{P}_{24}\hat{P}_{35})\times\frac{q_{3\mu}(q_4-q_5)_\lambda q_{2\sigma}}{D_{\rho 45}}. \quad (2.26)$$

In the above formulas, the superscript indicates the label of the corresponding figure. Once again, when obtaining $T^{(8)}_{\mu\lambda\sigma}$, the relation (2.12) is essential. A close inspection of Eq. (2.26) shows that the sum of the above tensors vanishes. Indeed, the cancellation of the ρ pole terms proportional to $c_1+c_2-c_3$ and of all the non-ρ-pole terms is evident. Let us check the cancellation of the ρ pole terms taking as an example the terms proportional to $q_\mu/6D_{\rho 25}$. One has for the sum of such terms the expression $3[q_{4\lambda}(q_2-q_5)_\sigma - q_{2\lambda}q_{5\sigma}]$. Applying the operator $1+\hat{P}_{34}$ and taking into account the four-momentum conservation and the presence of the tensor $\epsilon_{\mu\nu\lambda\sigma}$, one finds that the above combination vanishes. The cancellation of the remaining ρ pole terms is checked in the same manner. The cases of $q_{2,3,4}=0$ are obtained from the present case by Bose symmetry and by evident replacements of the pion momenta. In the case $q_5=0$, the contributions of the diagrams of Figs. 8, 9, and 10 vanish separately, while the contributions of the diagrams of Figs. 6 and 7 are equal in magnitude but opposite in sign, and hence they are canceled. The conditions for the vanishing of the amplitude in the Adler limit obtained in Sec. II A 1 and in this subsection turn out to be of great importance in obtaining the $\phi\to 5\pi$ decay amplitudes.

III. THE $\omega\to\pi^+\pi^-3\pi^0$ AND $\omega\to 2\pi^+2\pi^-\pi^0$ BRANCHING RATIOS RECONSIDERED

In our previous work Ref. [7], the branching ratios of the $\omega\to\pi^+\pi^-3\pi^0$ and $\omega\to 2\pi^+\pi^-\pi^0$ decays were estimated. Essential for that evaluation were the expressions for the contributions of the diagrams shown in Figs. 1 and 6, multiplied by the specific correction factors stemming from the diagrams shown in Figs. 2 and 7 of the present paper, respectively. This seemed to be justifiable because of the presence of the ρ pole. As will become clear later on, the non-ρ-pole terms are essential.

Strictly speaking, the HLS approach does not give *predictions* even for the $\omega\to\pi^+\pi^-\pi^0$ decay rate, because arbitrary constants $c_{1,2,3}$ enter the expression for the Lagrangian Eq. (1.9). As was pointed out in Refs. [1,2], these constants should be determined from experiment. Nevertheless, HLS relates the contributions to the amplitudes; compare Figs. 1 and 2 to Figs. 3, 4, and 5 (respectively, Figs. 6 and 7 to Figs. 8, 9, and 10), which otherwise appear unrelated. One can obtain reasonable predictions for the $\omega\to 5\pi$ decay rates upon assuming specific relations among the $c_{1,2,3}$. First, there are no experimental indications on the pointlike $\omega\to\pi^+\pi^-\pi^0$ vertex; hence one can take the relation Eq. (1.11) for granted. Second, the constant c_3 [see Eq. (1.12)], extracted from the $\omega\to 3\pi$ branching ratio, is remarkably close to unity. Note that older chiral models [3] for the vector meson interactions, added to the terms arising from gauging the anomalous Wess-Zumino action [5], predicted $c_3=1$. We fix c_3 from the $\omega\to 3\pi$ partial width [see Eqs. (1.10) and (1.12)]. After taking into account Eq. (1.11), the ratio c_1/c_3 remains arbitrary, and the magnitude of the $\omega\to 5\pi$ decay width depends on this parameter. We choose its value guided by the following considerations. Inspection of the expressions for the $\omega\to 5\pi$ decay amplitudes obtained in Sec. II shows that almost all the terms except those proportional to $c_1+c_2-c_3$, have the tensor structure

$$M=\frac{g_{\omega\rho\pi}g_{\rho\pi\pi}}{f_\pi^2}\varepsilon_{\mu\nu\lambda\sigma}q_\mu\epsilon_\nu T_{\lambda\sigma}, \quad (3.1)$$

where

$$T_{\lambda\sigma}=\sum_{a<b}G_{ab}q_{(a)\lambda}q_{(b)\sigma} \quad (3.2)$$

is a tensor composed of pion four-momenta $q_{(a)}$, $a=1,\ldots,5$, and G_{ab} are invariant amplitudes, whose explicit form can be read off the expressions for the amplitudes obtained in Sec. II by gathering the coefficients in front of $q_{(a)\lambda}q_{(b)\sigma}$. They are very lengthy, so we do not give them here. In the rest frame system of the decaying ω, the Lorentz structure of Eq. (3.1) is reduced to the three-dimensional form $e_{ijk}\xi_i T_{jk}$, where $\boldsymbol{\xi}$ is the polarization vector of the ω in this frame, and e_{ijk} is totally antisymmetric in $i,j,k=1,2,3$. This enormously simplifies the calculation of the modulus squared of the amplitude. In the meantime, all the terms proportional to $c_1+c_2-c_3$ have the four-dimensional tensor structure $\varepsilon_{\mu\nu\lambda\sigma}\epsilon_\mu q_{(a)\nu}q_{(b)\lambda}q_{(c)\sigma}$. The resulting expression for the modulus squared of the full amplitude turns out to be extremely lengthy. For the sake of simplicity, we set

$$c_1+c_2-c_3=0 \quad (3.3)$$

in what follows. Note that this means that the contributions of the diagrams of Figs. 5 and 10 together with part of the contributions from the diagrams of Figs. 4 and 9 are dropped. The results of relaxing the condition Eq. (3.3) are discussed at the end of the present section. Finally, our assumptions about the HLS arbitrary constants $c_{1,2,3}$ and a are

$$c_1=c_3,\ \ c_2=0,\ \ a=2. \quad (3.4)$$

Notice that the above relations among $c_{1,2,3}$ are the solutions of Eqs. (1.11) and (3.3).

The expression for the partial width of the decays (1.1) and (1.2) is

$$\Gamma_{\omega\to 5\pi}(s)=\frac{1}{2\sqrt{s}(2\pi)^{11}N_{\rm sym}}\int|M|^2 d\mathcal{D}_5, \quad (3.5)$$

where $s=(\Sigma_{a=1}^5 q_a)^2$ is the total energy squared in the rest frame system of the decaying particle, the Bose symmetry factor $N_{\rm sym}=6,4$ for the reactions (1.1), (1.2), respectively, and $d\mathcal{D}_5$ given in Ref. [9] is the differential element of the phase space volume of the five-pion final state. Note that we take into account the mass difference of the charged and

neutral pions both in the amplitude and in the phase space volume. In the above formula,

$$|M|^2=\frac{1}{3}\left(\frac{g_{\omega\rho\pi}g_{\rho\pi\pi}}{f_\pi^2}\right)^2\frac{s}{2}\sum_{i,j=1}^{3}|T_{ij}-T_{ji}|^2 \qquad (3.6)$$

is the modulus squared of the amplitude Eq. (3.1) averaged over three independent polarizations of the ω. When evaluating Eq. (3.5), the eight Mandelstam-like invariant variables $s_i, u_i, i=1,2,3,$ and t_1, t_2 proposed by Kumar in Ref. [9] are suitable. They are given in the Appendix. All the scalar products of the pair of pion four-momenta are expressed via the Kumar variables by expressions given in the Appendix. For numerical evaluation of the eight-dimensional integral over Kumar variables we use the method suggested in Ref. [10].

We evaluate both the branching ratios for the two mentioned isotopic modes at the resonance mass,

$$B_{\omega\to5\pi}(m_\omega^2)=\frac{\Gamma_{\omega\to5\pi}(m_\omega^2)}{\Gamma_\omega}, \qquad (3.7)$$

and the branching ratios averaged over the resonance peak,

$$B^{\rm av}_{\omega\to5\pi}=\frac{2}{\pi}\int_{\sqrt{s}=m_\omega-\Gamma_\omega}^{\sqrt{s}=m_\omega+\Gamma_\omega}d\sqrt{s}\frac{s\Gamma_{\omega\to5\pi}(s)}{(s-m_\omega^2)^2+m_\omega^2\Gamma_\omega^2}. \qquad (3.8)$$

The quantity $B^{\rm av}_{\omega\to5\pi}$ is useful in situations where the total energy of the five-pion state is not directly measured, as is the case in, e.g., photoproduction or peripheral production in πN collisions. The results of the evaluation are the following:

$$B_{\omega\to\pi^+\pi^-3\pi^0}(m_\omega^2)=3.6\times10^{-9},$$

$$B^{\rm av}_{\omega\to\pi^+\pi^-3\pi^0}=2.8\times10^{-9},$$

$$B_{\omega\to2\pi^+2\pi^-\pi^0}(m_\omega^2)=3.5\times10^{-9},$$

$$B^{\rm av}_{\omega\to2\pi^+2\pi^-\pi^0}=2.7\times10^{-9}. \qquad (3.9)$$

These branching ratios for the $\omega\to5\pi$ decay exceed those obtained in our previous paper Ref. [7] by a factor of more than 3. The reason for the disagreement is the following. As mentioned at the beginning of the present section, the diagrams of Figs. 1 and 6 corrected with those of Figs. 2 and 7 were considered to be dominant in Ref. [7]. Let us evaluate the contributions of the diagrams of Figs. 1 and 6 to the branching ratios of the decays $\omega\to\pi^+\pi^-3\pi^0$ and $\omega\to2\pi^+2\pi^-\pi^0$, respectively. For a reason soon to become clear in the case of the $\phi\to5\pi$ decay, we call these contributions resonant. One obtains $B^{\rm resonant}_{\omega\to\pi^+\pi^-3\pi^0}=1.54\times10^{-9}$ and $B^{\rm resonant}_{\omega\to2\pi^+2\pi^-\pi^0}=1.4\times10^{-9}$. These figures are close to $B_{\omega\to\pi^+\pi^-3\pi^0}\simeq B_{\omega\to2\pi^+\pi^-\pi^0}\simeq1\times10^{-9}$ obtained in Ref. [7]. The evaluation of the net contribution of all the remaining diagrams (called nonresonant) gives $B^{\rm nonresonant}_{\omega\to\pi^+\pi^-3\pi^0}=0.47\times10^{-9}$ and $B^{\rm nonresonant}_{\omega\to\pi^+\pi^-3\pi^0}=0.50\times10^{-9}$. The nonresonant contributions amount to 13–14 % of the total Eq. (3.9). However, the phase space averaged relative phase difference between the resonant and nonresonant contributions evaluated with the above numbers is $\delta=21°$ and $\delta=17°$, respectively, for the reactions (1.1) and (1.2). These phase differences and the comparison with the total branching ratios Eq. (3.9) show that the mentioned contributions to the decay amplitude are almost in phase. The neglect of seemingly small nonresonant contributions resulted in the underestimated magnitude of the branching ratios in Ref. [7].

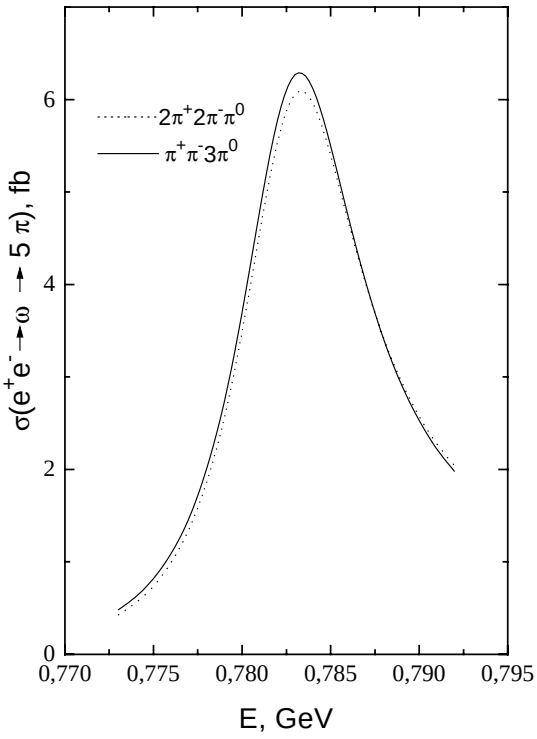

FIG. 11. The excitation curve of the decays $\omega\to5\pi$ in e^+e^- annihilation.

The excitation curves for the $\omega\to5\pi$ decays in e^+e^- annihilation,

$$\sigma_{\omega\to5\pi}(s)=12\pi\left(\frac{m_\omega}{\sqrt{s}}\right)^3\Gamma_{\omega\to e^+e^-}(m_\omega^2)\frac{s\Gamma_{\omega\to5\pi}(s)}{(s-m_\omega^2)^2+m_\omega^2\Gamma_\omega^2}, \qquad (3.10)$$

are plotted in Fig. 11. The curves are asymmetric and shifted by 0.7 MeV toward higher values from the ω mass because of the strong energy dependence of $\Gamma_{\omega\to5\pi}(s)$ (see Fig. 12 below). As is seen, the two isotopic channels have approximately equal branching ratios and almost coincident excitation curves in the ω resonance region. This can be understood as follows. The matrix elements squared are numerically approximately the same in the near-to-threshold region, since the pion mass difference is smeared in the sum of various contributions. Hence, they are canceled in the ratio of the two partial widths, leaving the ratio of the phase space volumes. Using the nonrelativistic expression for the phase space volume of the five-pion final state from Ref. [11], one obtains

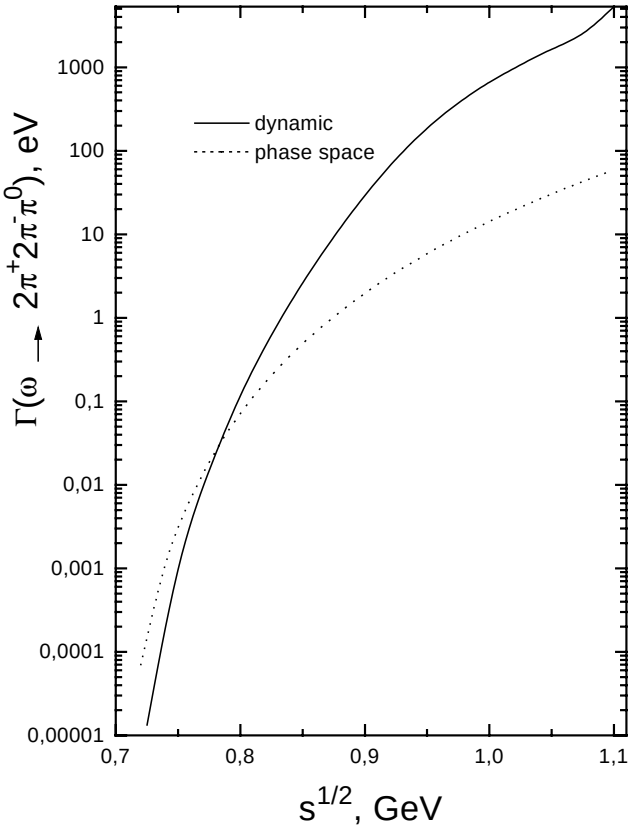

FIG. 12. The energy dependence of the $\omega\to 2\pi^+2\pi^-\pi^0$ partial width.

$$\frac{B(\omega\to 2\pi^+2\pi^-\pi^0,m_\omega^2)}{B(\omega\to\pi^+\pi^-3\pi^0,m_\omega^2)} = \frac{3m_{\pi^+}}{2m_{\pi^0}}\left(\frac{2m_{\pi^+}+3m_{\pi^0}}{4m_{\pi^+}+m_{\pi^0}}\right)^{3/2}\left(\frac{m_\omega-4m_{\pi^+}-m_{\pi^0}}{m_\omega-2m_{\pi^+}-3m_{\pi^0}}\right)^5 = 0.93, \tag{3.11}$$

to be compared to 0.96 calculated from Eq. (3.9). The ratio of the Bose symmetry factors 3/2 compensates the smaller-phase space volume of the final state $2\pi^+2\pi^-\pi^0$ as compared to $\pi^+\pi^-3\pi^0$. In the meantime, the energy dependence of the $\omega\to 5\pi$ partial width in the dynamical model is drastically different from that in the model of the Lorentz-invariant phase space (LIPS). In the latter, one has the following expression for the $\omega\to 5\pi$ partial width:

$$\Gamma^{(\mathrm{LIPS})}_{\omega\to 5\pi}(s)=\Gamma_{\omega\to 5\pi}(m_\omega^2)\frac{W_{5\pi}(s)}{W_{5\pi}(m_\omega^2)}, \tag{3.12}$$

where $\Gamma_{\omega\to 5\pi}(m_\omega^2)$ is the partial width evaluated with the dynamical amplitudes given in Sec. II, and the expression for the Lorentz invariant phase space volume is

$$W_{5\pi}(s)=\frac{\pi^4}{(2\pi)^{11}32s^{3/2}N_{\mathrm{sym}}}\int_{(m_1+m_2+m_3+m_4)^2}^{(\sqrt{s}-m_5)^2}\frac{ds_1}{s_1}\lambda^{1/2} \times(s,s_1,m_5^2)\int_{(m_1+m_2+m_3)^2}^{(\sqrt{s_1}-m_4)^2}\frac{ds_2}{s_2}\lambda^{1/2}(s_1,s_2,m_4^2) \times\int_{(m_1+m_2)^2}^{(\sqrt{s_2}-m_3)^2}\frac{ds_3}{s_3}\lambda^{1/2}(s_2,s_3,m_3^2)\lambda^{1/2}(s_3,m_1^2,m_2^2), \tag{3.13}$$

with m_i, $i=1,\ldots,5$, being the mass of the meson π_i, and

$$\lambda(x,y,z)=x^2+y^2+z^2-2xy-2xz-2yz. \tag{3.14}$$

The predictions of both models for the energy dependence of $\Gamma_{\omega\to 2\pi^+2\pi^-\pi^0}(s)$ are plotted in Fig. 12. The plot for the $\pi^+\pi^-3\pi^0$ final state looks similar and is not given here. The faster growth of the partial width in the dynamical as compared to the phase space model is due to the resonance enhancement arising from the opening of ρ production in the intermediate state.

Let us relax the constraint Eq. (3.3) on the parameters $c_{1,2,3}$. To be specific, we choose $-2\leqslant c_2\leqslant 2$ instead of $c_2=0$ assumed earlier. The corresponding ratio $\gamma=(c_1+c_2-c_3)/4c_3$ parametrizing the strength of the neglected terms then falls into the interval $-1\leqslant\gamma\leqslant 1$ or $-1\leqslant c_1/c_3\leqslant 3$. The branching ratios $B_{\omega\to 5\pi}$ evaluated with the new parameters deviate by less than 1% from those evaluated at $\gamma=0$.

IV. THE EVALUATION OF THE $\phi\to\pi^+\pi^-3\pi^0$ AND $\phi\to 2\pi^+2\pi^-\pi^0$ BRANCHING RATIOS

As is known, chiral models, including HLS, do not possess terms responsible for the decays of ϕ mesons into final states containing nonstrange quarks only. However, one can guess the general form of such terms guided by both the OZI rule violation in the decay $\phi\to\rho\pi\to\pi^+\pi^-\pi^0$ and by the Adler condition.

There are two feasible models of the OZI-suppressed $\phi\to\rho\pi$ decay amplitude. The first one is the $\phi\omega$ mixing model, where the above decay proceeds due to the small admixture of nonstrange quarks in the flavor wave function of the ϕ meson composed mostly of a pair of strange quarks. In the second model ϕ goes to $\rho\pi$ directly (see Ref. [12]). Earlier, we pointed out that there are no particular reasons to prefer one model to another, and possible ways to resolve the issue were pointed out in [12,13]. Recent SND data [14] point to a sizable coupling constant of direct $\phi\to\rho\pi$ transition, assuming the dependence $|\psi(0,m_V)|^2\propto m_V^2$ [12] of the wave function of the vector $q\bar{q}$ bound state at the origin on the mass m_V of this state. It should be noted that the assumed dependence agrees remarkably well with the ratios of the measured leptonic widths of the vector quarkonia ρ, ω, ϕ, J/ψ, and $\Upsilon(1S)$.

The decays $\phi\to 5\pi$ are treated slightly differently in the above models of OZI rule violation. Let us consider them in due turn. In the model of $\phi\omega$ mixing ϕ goes to the off-mass-

shell ω, which decays as considered in Sec. II. Hence, one can immediately obtain

$$\Gamma_{\phi\to 5\pi}(m_\phi^2)=|\varepsilon_{\phi\omega}(m_\phi^2)|^2\Gamma_{\omega\to 5\pi}(m_\phi^2), \tag{4.1}$$

where $\varepsilon_{\phi\omega}(m_\phi)$ is the complex parameter of $\phi\omega$ mixing taken at the ϕ mass. It can be evaluated as

$$|\varepsilon_{\phi\omega}(m_\phi^2)|^2=\frac{\Gamma_{\phi\to 3\pi}(m_\phi^2)}{\Gamma_{\omega\to 3\pi}(m_\omega^2)}\cdot r=3.04\times 10^{-3},$$

where $r=3.5\times 10^{-2}$ is the ratio of the three-pion phase space volumes at the ω and ϕ peaks.

If $\phi\omega$ mixing is negligible, one should introduce a number of new OZI rule violating parameters to quantify the $\phi\to 5\pi$ decay amplitude. Guided by the condition of chiral symmetry expressed as the demand that the correct decay amplitude should satisfy the Adler condition, it is reasonable to expect that the effective Lagrangian describing anomalous OZI suppressed decays of ϕ mesons looks similar to the Lagrangian Eq. (1.9),

$$\begin{aligned}\mathcal{L}^{\rm an}_{\phi,\rho,\pi}=&\frac{1}{2f_\pi^3}(\beta_1-\beta_2-\beta_3)\varepsilon_{\mu\nu\lambda\sigma}\phi_\mu(\partial_\nu\boldsymbol{\pi}\cdot[\partial_\lambda\boldsymbol{\pi}\times\partial_\sigma\boldsymbol{\pi}])+\frac{1}{8f_\pi^5}\left[-\beta_1+\frac{5}{3}(\beta_2+\beta_3)\right]\varepsilon_{\mu\nu\lambda\sigma}\phi_\mu(\partial_\nu\boldsymbol{\pi}\cdot[\partial_\lambda\boldsymbol{\pi}\times\partial_\sigma\boldsymbol{\pi}])\boldsymbol{\pi}^2\\&-\frac{2\beta_3 g}{f_\pi}\varepsilon_{\mu\nu\lambda\sigma}\partial_\mu\phi_\nu\left\{(\boldsymbol{\rho}_\lambda\cdot\partial_\sigma\boldsymbol{\pi})+\frac{1}{6f_\pi^2}[(\boldsymbol{\rho}_\lambda\cdot\boldsymbol{\pi})(\boldsymbol{\pi}\cdot\partial_\sigma\boldsymbol{\pi})-\boldsymbol{\pi}^2(\boldsymbol{\rho}_\lambda\cdot\partial_\sigma\boldsymbol{\pi})]\right\}-\frac{2g}{f_\pi}(\beta_1+\beta_2\\&-\beta_3)\varepsilon_{\mu\nu\lambda\sigma}\phi_\mu\left\{\frac{1}{4f_\pi^2}(\partial_\nu\boldsymbol{\pi}\cdot\boldsymbol{\rho}_\lambda)(\boldsymbol{\pi}\cdot\partial_\sigma\boldsymbol{\pi})-\frac{g}{4}([\boldsymbol{\rho}_\nu\times\boldsymbol{\rho}_\lambda]\cdot\partial_\sigma\boldsymbol{\pi})\right\},\end{aligned} \tag{4.2}$$

where $\beta_{1,2,3}$ are the above mentioned parameters responsible for the violation of the OZI rule in the $\phi\to 5\pi$ decays of ϕ mesons. An analysis similar to that presented in Secs. II A 1 and II B 1 shows that the $\phi\to 5\pi$ decay amplitudes obtained from the Lagrangian (4.2) satisfy the Adler condition. As is evident from Eq. (4.2), one should identify the coupling constant of direct $\phi\to\rho\pi$ transition as

$$g_{\phi\rho\pi}=-\frac{2\beta_3 g}{f_\pi}=0.8\ \ \mathrm{GeV}^{-1}, \tag{4.3}$$

where the magnitude of $g_{\phi\rho\pi}$ is obtained from the $\phi\to 3\pi$ partial widths, while the positive sign (relative to $g_{\omega\rho\pi}$ usually taken to be positive) is fixed by the $\phi\omega$ interference pattern observed in the energy dependence of the $e^+e^-\to\pi^+\pi^-\pi^0$ reaction cross section [15]. Note that we neglect the unitarity corrections to $g_{\phi\rho\pi}$ [16], because they are irrelevant in the context of the present work. Next, there seems to be no sizable pointlike $\phi\to\pi^+\pi^-\pi^0$ contribution. Indeed, first, the existing upper limit to the branching ratio of the non-$\rho\pi$ intermediate state direct transition $\phi\to\pi^+\pi^-\pi^0$ obtained by the SND group at VEPP-2M is very small [17],

$$B^{\rm direct}(\phi\to\pi^+\pi^-\pi^0)<6\times 10^{-4}(90\%\ \mathrm{C.L.}). \tag{4.4}$$

Second, the KLOE Collaboration at DAΦNE gives the phase space averaged direct $\phi\to\pi^+\pi^-\pi^0$ contribution at the level of 1% [18] of the total $\pi^+\pi^-\pi^)$ decay rate. Hence, in close analogy with the ω case, one can set

$$\beta_1-\beta_2-\beta_3=0. \tag{4.5}$$

The results of relaxing these conditions are discussed at the end of the present section. The magnitude $\beta_3=-0.006$ is fixed according to Eq. (4.3) by the $\phi\to 3\pi$ partial widths. Finally, the ratio β_1/β_3 remains arbitrary. We set

$$\beta_1+\beta_2-\beta_3=0, \tag{4.6}$$

and hence $\beta_1=\beta_3$, $\beta_2=0$, so that the $\phi\to 5\pi$ decay amplitudes are determined only by the parameter β_3 and look like Eq. (3.1) for the $\omega\to 5\pi$ decay, with the replacement $g_{\omega\rho\pi}\to g_{\phi\rho\pi}$. The tensor $T_{\lambda\sigma}$ is the same as in the $\omega\to 5\pi$ decay amplitude. Under these assumptions both mentioned models for the OZI rule violating decay $\phi\to 3\pi$ give similar results for the branching ratios of the decays $\phi\to 5\pi$. These are the following:

$$\begin{aligned}B_{\phi\to\pi^+\pi^-3\pi^0}(m_\phi^2)&=2.4\times 10^{-7},\\ B^{\rm av}_{\phi\to\pi^+\pi^-3\pi^0}&=1.8\times 10^{-7},\\ B_{\phi\to 2\pi^+2\pi^-\pi^0}(m_\phi^2)&=6.9\times 10^{-7},\\ B^{\rm av}_{\phi\to 2\pi^+2\pi^-\pi^0}&=4.9\times 10^{-7},\end{aligned} \tag{4.7}$$

where $B^{\rm av}$, useful for the reactions of peripheral production, stands for the branching ratio averaged over the $\pm\Gamma_\phi$ region around the ϕ peak [use Eq. (3.8) with the replacement $\omega\to\phi$]. The evaluation of the excitation curve of the decays $\phi\to 5\pi$ in e^+e^- annihilation performed according to Eq. (3.10) (with the replacement $\omega\to\phi$) is plotted in Fig. 13. Notice that the ratio of the branching ratios of the two isotopic modes at the ϕ peak is

$$\frac{B_{\phi\to 2\pi^+2\pi^-\pi^0}(m_\phi^2)}{B_{\phi\to\pi^+\pi^-3\pi^0}(m_\phi^2)}=2.9, \tag{4.8}$$

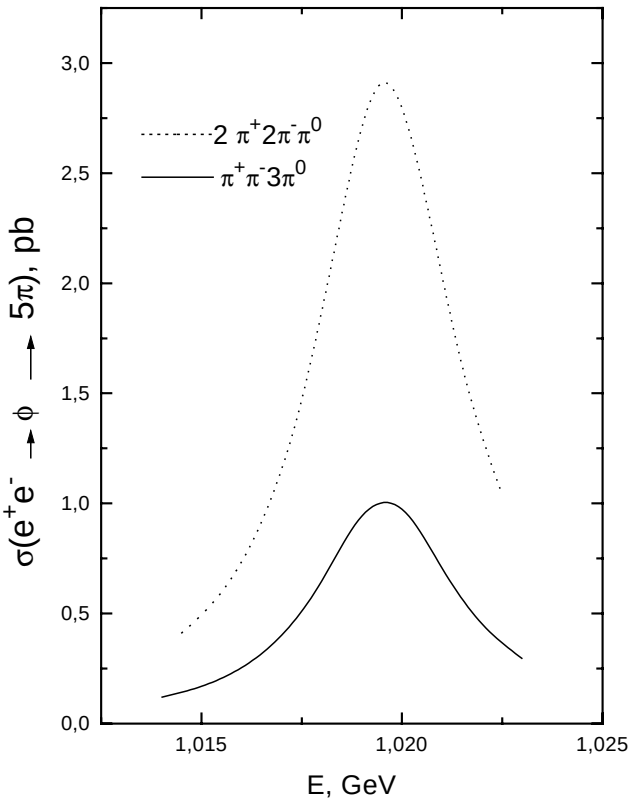

FIG. 13. The excitation curve of the decays $\phi\to 5\pi$ in e^+e^- annihilation.

to be compared to the figure of 1.3 obtained from a simple evaluation of the ratio of the nonrelativistic phase spaces [see Eq. (3.11) with the replacement $m_\omega\to m_\phi$]. In the present case, the difference from the exact evaluation is sizable, because now the phase space model is inadequate due to the strong ρ and ω ($\rho\to\omega\pi\to 4\pi$) resonance production in the intermediate states. The $\phi\to 5\pi$ excitation curve is plotted in Fig. 13.

In this respect, it is interesting to look at the dynamical behavior of the specific contributions to the $\phi\to 5\pi$ decay amplitudes in another way. Let us evaluate, for this purpose, the contribution to $B_{\phi\to\pi^+\pi^-3\pi^0}$ of the diagrams of Fig. 1, at the ϕ mass. (Notice that now ω in the initial state should be replaced by ϕ in all the diagrams, and the effective $g_{\phi\rho\pi}$ is understood as the corresponding expression, while other couplings are related to it as explained earlier in this section.) The ρ meson in these diagrams is resonant. Indeed, choosing the averaged pion energy from the condition of equilibrium as $\langle E_\pi\rangle = m_\phi/5$, one finds that the invariant mass of four pions emitted in the transition $\rho\to 4\pi$ is $m_{4\pi}\simeq m_\rho$. The evaluation gives $B^{\rm resonant}_{\phi\to\pi^+\pi^-3\pi^0}=2.1\times 10^{-7}$. All the remaining contributions with the nonresonant intermediate ρ meson (see Figs. 2–4) amount to $B^{\rm nonresonant}_{\phi\to\pi^+\pi^-3\pi^0}=0.34\times 10^{-7}$, which constitutes 16% of the resonant contribution. Notice that the seemingly resonant diagrams of Figs. 2 and 7 do not, in fact, possess this property, because the three pions produced from the transition $\pi\to 3\pi$ push the ρ meson away from resonance. Indeed, the invariant mass of the pion pair in the transition $\rho\to 2\pi$ evaluated assuming the same average pion energy as above falls into the interval $2m_\pi\leqslant m_{2\pi}\leqslant 0.41$ GeV, which is far from the resonance value. The phase space averaged relative phase between the resonant and nonresonant contributions calculated with the help of the given branching ratios and those given in Eq. (4.7) is about $\delta=91°$. Correspondingly, similar calculations for the other isotopic state $2\pi^+2\pi^-\pi^0$ state give $B^{\rm resonant}_{\phi\to 2\pi^+2\pi^-\pi^0}=6.2\times 10^{-7}$ from Fig. 6, $B^{\rm nonresonant}_{\phi\to 2\pi^+2\pi^-\pi^0}=0.70\times 10^{-7}$ from Figs. 7–9, and $\delta=89°$. In the present case, the nonresonant contribution constitutes about 11% of the resonant one. The above estimates illustrate clearly the dominance of the diagrams with a resonant ρ meson in the intermediate state in the decay $\phi\to 5\pi$, because the resonant and the smaller nonresonant contributions add incoherently in the case of the $\phi\to 5\pi$ decay. For comparison, the opposite situation takes place in the case of the $\omega\to 5\pi$ decay amplitudes (see the corresponding calculations in Sec. III), where the smaller nonresonant contribution to the decay amplitude adds almost in phase with the resonant one and for this reason is essential.

Relaxing the constraint Eq. (4.6) to $-1\leqslant(\beta_1+\beta_2-\beta_3)/4\beta_3\leqslant 1$, analogous to that discussed in the ω case, implies even smaller deviations of $B_{\phi\to 5\pi}$ in comparison with the ω case, because the terms in the amplitude that are sensitive to the parameter in the above inequality are almost incoherent with the dominant ones. On the other hand, relaxing the constraint of the absence of pointlike $\phi\to\pi^+\pi^-\pi^0$ amplitude [see Eq. (4.5)] gives the following. Using the KLOE data Ref. [18], one can estimate the combination characterizing the pointlike $\phi\to\pi^+\pi^-\pi^0$ vertex as $|3(\beta_1-\beta_2-\beta_3)/2\beta_3 m_\rho^2|\simeq 1$. The evaluation of $B_{\phi\to 5\pi}$, keeping the constraint Eq. (4.6), gives results deviating by $\pm 8\%$ (depending on the sign of the above combination) from those obtained under the constraint Eq. (4.5).

The whole discussion above shows that the branching ratios of the decays $\phi\to\pi^+\pi^-3\pi^0$ and $\phi\to 2\pi^+2\pi^-\pi^0$ are determined within the conservatively estimated accuracy 20% by the well studied OZI rule violating transition of ϕ mesons to the $\rho\pi$ state followed by the transition $\rho\to 4\pi$ in a model independent way.

V. DISCUSSION AND CONCLUSION

In view of the fact that there are three (or even four, if one includes radiative decays; see Ref. [1,2]) independent constants in the effective chiral Lagrangian describing anomalous decays of ω (and ϕ) mesons, one can consider only some scenarios of what may happen. We restrict ourselves to considering only the strong decays. In principle, a study of the Dalitz plot in $\omega\to\pi^+\pi^-\pi^-$ decay allows one to extract c_3 and $(c_1-c_2)/c_3$ by isolating the ρ pole and non-ρ-pole contributions, because the density on this plot is proportional, omitting the $\omega\rho$ interference term in the $\pi^+\pi^-$ mass spectrum, to the factor

$$\frac{d^2N}{dm_+dm_-}\propto\left|\frac{1}{D_\rho(q_1+q_2)}+\frac{1}{D_\rho(q_1+q_3)}+\frac{1}{D_\rho(q_2+q_3)}+3\frac{c_1-c_2-c_3}{2c_3m_\rho^2}\right|^2, \quad (5.1)$$

where $m_+^2=(q_1+q_3)^2$, $m_-^2=(q_2+q_3)^2$. Notice in this respect that the combination of parameters of the low energy effective Lagrangian entering in the non-ρ-pole term in Eq. (5.1) should be treated as the low energy limit of all possible contributions from the transitions $\omega\to\rho'\pi$, $\rho''\pi$, etc. If one assumes that direct transitions are responsible for the decays of ϕ mesons to states containing no strange quarks, the same will be true for the parameters $\beta_{1,2,3}$ characterizing the OZI rule violating decays $\phi\to3\pi$ and $\phi\to5\pi$. In the model of $\phi\omega$ mixing, the $\phi\to5\pi$ decay amplitude contains no additional free parameters as compared to the case of $\omega\to5\pi$ decay. It should be recalled that the two models can, in principle, be discriminated by careful study of the $\phi\omega$ interference minimum in the energy dependence of the $e^+e^-\to\pi^+\pi^-\pi^0$ reaction cross section or by the ratio of the leptonic widths of the ω and ϕ mesons [12–14]. On the other hand, within an accuracy of 20%, the branching ratios of the $\phi\to5\pi$ decays can be evaluated in a model independent way; see the discussion at the end of Sec. IV.

The excitation curves of the decays $\omega\to5\pi$ and $\phi\to5\pi$ in e^+e^- annihilation can be used to evaluate the expected number of these decays at the ω and ϕ peaks. With the luminosity $L=10^{32}\ \mathrm{cm}^{-2}\,\mathrm{s}^{-1}$ at the ω peak, one may hope to observe three events of the decays $\omega\to\pi^+\pi^-3\pi^0$ and $2\pi^+2\pi^-\pi^0$ per each mode bimonthly. With the same luminosity at the ϕ peak, the observation of 750 (250) $\phi\to2\pi^+2\pi^-\pi^0$ ($\phi\to\pi^+\pi^-3\pi^0$) decays per month is feasible. Note that the existing upper limit is $B_{\phi\to2\pi^+2\pi^-\pi^0}<4.6\times10^{-6}$ (90% C.L.) [19]. With the luminosity $L=500\ \mathrm{pb}^{-1}$ already attained at the ϕ factory DAΦNE [22], one could gain about 1685 events of the decay $\phi\to5\pi$ proceeding via chiral mechanisms considered in the present paper. The possible non-chiral-model background from the dominant decay $\phi\to K_LK_S$, $K_L\to3\pi$, $K_S\to2\pi$ is well separated from the considered chiral mechanism by the macroscopic distances that kaons move away to. The rare decay $\phi\to\eta\pi^+\pi^-$, whose branching ratio was estimated [20,21] at the level $B_{\phi\to\eta\pi^+\pi^-}\sim3\times10^{-7}$, is cut by removing events in the vicinity of the η peak in the three-pion distribution observed in the five-pion events [19].

In the present work, we neglect the contribution of the $a_1(1260)$ meson. This is justifiable because both the $\omega(782)$ and $\phi(1020)$ peaks are deep under the threshold of $a_1\pi$ production. As is known, the approach to chiral dynamics based on HLS allows one to take the axial vector mesons into account [1,2]. This is the theme of future work.

ACKNOWLEDGMENTS

The present study was partially supported by the grant RFFI-02-02-16061 from the Russian Foundation for Basic Research.

APPENDIX: RELATIONS EXPRESSING LORENTZ SCALAR PRODUCTS THROUGH THE KUMAR VARIABLES

In this appendix, the relations expressing the Lorentz scalar products (q_i,q_j) through Lorentz invariant variables are presented. Given the pion momentum assignment according to

$$\omega_q\to\pi_{q_1}\pi_{q_2}\pi_{q_3}\pi_{q_4}\pi_{q_5}, \quad (A1)$$

the eight Kumar variables [9] are defined as

$$\begin{aligned}
s_1&=(q-q_1)^2,\\
s_2&=(q-q_1-q_2)^2,\\
s_3&=(q-q_1-q_2-q_3)^2,\\
u_1&=(q-q_2)^2,\\
u_2&=(q-q_3)^2,\\
u_3&=(q-q_4)^2\\
t_2&=(q-q_2-q_3)^2,\\
t_3&=(q-q_2-q_3-q_4)^2.
\end{aligned} \quad (A2)$$

Associated with them, but not independent, are the following:

$$\begin{aligned}
s_2'&=(q_1+q_2)^2,\\
s_3'&=(q_1+q_2+q_3)^2,\\
s_4'&=(q-q_5)^2,\\
t_2'&=(q_2+q_3)^2,\\
t_3'&=(q_2+q_3+q_4)^2.
\end{aligned} \quad (A3)$$

Then the greater part of the Lorentz scalar products of the pion momenta can be expressed through the variables Eq. (A2) and (A3):

$$\begin{aligned}
(q_1,q_2)&=\frac{1}{2}(s_2'-m_1^2-m_2^2),\\
(q_1,q_3)&=\frac{1}{2}(s_3'-s_2'-t_2'+m_2^2),\\
(q_1,q_4)&=\frac{1}{2}(t_2-t_3-s_3+m_5^2),\\
(q_1,q_5)&=\frac{1}{2}(t_3-m_1^2-m_5^2),\\
(q_2,q_3)&=\frac{1}{2}(t_2'-m_2^2-m_3^2),\\
(q_4,q_5)&=\frac{1}{2}(s_3-m_4^2-m_5^2).
\end{aligned} \quad (A4)$$

The remaining scalar products

$$(q_3,q_5)=\frac{1}{2}(s_2-s_3-m_3^2)-(q_3,q_4),$$

$$(q_2,q_4)=\frac{1}{2}(t_3'-t_2'-m_4^2)-(q_3,q_4) \tag{A5}$$

can be expressed through (q_3,q_4). The latter, using the method of invariant integration outlined in Appendix D of Ref. [9], can be found as

$$(q_3,q_4)=\frac{1}{2}[\alpha(s-u_2+m_3^2)+\beta(u_1-t_2-m_3^2)+\gamma(s_2-s_3-m_3^2)], \tag{A6}$$

where

$$\alpha=\frac{1}{\Delta_M}(Ft_2s_3+BCG+ACH-t_2BH-C^2F-As_3G),$$

$$\beta=\frac{1}{\Delta_M}(ss_3G+ABH+BCF-B^2G-sCH-As_3F),$$

$$\gamma=\frac{1}{\Delta_M}(st_2H+ABG+ACF-t_2BF-sCG-A^2H), \tag{A7}$$

and

$$A=\frac{1}{2}(s+t_2-t_2'),$$

$$B=\frac{1}{2}(s+s_3-s_3'),$$

$$C=\frac{1}{2}(s_3+t_2-m_1^2),$$

$$F=\frac{1}{2}(s-u_3+m_4^2),$$

$$G=\frac{1}{2}(t_2-t_3+m_4^2),$$

$$H=\frac{1}{2}(s_3+m_4^2-m_5^2),$$

$$\Delta_M=st_2s_3+2ABC-B^2t_2-C^2s-A^2s_3. \tag{A8}$$

In the above formulas, m_i, $i=1,\ldots,5$, are the masses of the final pions.

[1] M. Bando *et al.*, Phys. Rev. Lett. **54**, 1215 (1985); M. Bando, T. Kugo, and K. Yamawaki, Nucl. Phys. **B259**, 493 (1985); Prog. Theor. Phys. **73**, 1541 (1985); Phys. Rep. **164**, 217 (1988).

[2] M. Harada and K. Yamawaki, Phys. Rep. **381**, 1 (2003).

[3] Ö. Kaymakcalan, S. Rajeev, and J. Schechter, Phys. Rev. D **30**, 594 (1984).

[4] K. Kawarabayashi and M. Suzuki, Phys. Rev. Lett. **16**, 255 (1966); Riazzuddin and Fayyazuddin, Phys. Rev. **147**, 1071 (1966).

[5] J. Wess and B.B. Zumino, Phys. Lett. **37B**, 95 (1971).

[6] Particle Data Group, K. Hagiwara *et al.*, Phys. Rev. D **66**, 010001 (2002).

[7] N.N. Achasov and A.A. Kozhevnikov, Phys. Rev. D **62**, 056011 (2000); Zh. Éksp. Teor. Fiz. **91**, 499 (2000) [JETP **91**, 433 (2000)].

[8] S. Weinberg, Phys. Rev. **166**, 1568 (1968).

[9] R. Kumar, Phys. Rev. **185**, 1865 (1969).

[10] T.W. Sag and G. Szekeres, Math. Comput. **18**, 245 (1964).

[11] E. Byckling and K. Kajantie, *Particle Kinematics* (Wiley, London, 1973).

[12] N.N. Achasov and A.A. Kozhevnikov, Phys. Rev. D **52**, 3119 (1995); Yad. Fiz. **59**, 153 (1996) [Phys. At. Nucl. **59**, 144 (1996)].

[13] N.N. Achasov and A.A. Kozhevnikov, Yad. Fiz. **55**, 3086 (1992) [Sov. J. Nucl. Phys. **55**, 1726 (1992)]; Part. World **3**, 125 (1993).

[14] M.N. Achasov *et al.*, Phys. Rev. D **68**, 052006 (2003).

[15] M.N. Achasov *et al.*, Phys. Rev. D **63**, 072002 (2001).

[16] N.N. Achasov and A.A. Kozhevnikov, Phys. Rev. D **61**, 054005 (2000); Yad. Fiz. **63**, 2029 (2000) [Phys. At. Nucl. **63**, 1936 (2000)].

[17] M.N. Achasov *et al.*, Phys. Rev. D **65**, 032002 (2002).

[18] KLOE Collaboration, A. Aloisio *et al.*, Phys. Lett. B **561**, 55 (2003).

[19] R.R. Akhmetshin *et al.*, Phys. Lett. B **491**, 81 (2000).

[20] N.N. Achasov and V.A. Karnakov, JETP Lett. **39**, 342 (1984).

[21] N.N. Achasov and A.A. Kozhevnikov, Int. J. Mod. Phys. A **7**, 4825 (1992); Yad. Fiz. **55**, 809 (1992) [Sov. J. Nucl. Phys. **55**, 449 (1992)].

[22] KLOE Collaboration, A. Passeri, ''Recent Results from the KLOE Experiment at DAΦNE,'' hep-ex/0305108.